energies

MDPI

Article

Change of the Properties of Steel Material of the Roller Cone Bit Due to the Influence of the Drilling Operational Parameters and Rock Properties

Jurij Šporin [1,*], Tilen Balaško [2], Primož Mrvar [2], Blaž Janc [1] and Željko Vukelić [1]

[1] Department of Geotechnology, Mining and Environment, Faculty of Natural Sciences and Engineering, University of Ljubljana, Aškerčeva 12, 1000 Ljubljana, Slovenia; blaz.janc@ogr.ntf.uni-lj.si (B.J.); zeljko.vukelic@ogr.ntf.uni-lj.si (Ž.V.)

[2] Department of Materials and Metallurgy, Faculty of Natural Sciences and Engineering, University of Ljubljana, Aškerčeva 12, 1000 Ljubljana, Slovenia; tilen.balasko@ntf.uni-lj.si (T.B.); primoz.mrvar@ntf.uni-lj.si (P.M.)

* Correspondence: jurij.sporin@ogr.ntf.uni-lj.si; Tel.: +386-1-47-04-619

Received: 12 October 2020; Accepted: 10 November 2020; Published: 14 November 2020



Abstract: The breakdown of the drill bit or rapid decrease of the rate of penetration during the drilling process results in a delay in the progress of drilling. Scientists and engineers are increasingly focusing on research to extend the bit life and improve the drilling rate. In our work, "in situ" drilling parameters were monitored during the drilling process with the roller cone drill bit IADC 136, diameter 155.57 mm (6 1/8"). After drilling, the bit was thoroughly examined to determine the damage and wear that occurred during drilling. The following modern and standardized investigative methods were used: an analysis of rock materials and an analysis of micro and macrostructure materials of the roller cone bit. Analyses were carried out using optical and electron microscopy, a simultaneous thermal analysis of materials of drill bit, analysis of the chemical composition of materials of drill bit, and a determination of the geomechanical parameters of rock materials. The resulting wear, local bursts, and cracks were quantitatively and qualitatively defined and linked to the drilling regime and the rock material. The results of our investigation of the material of the roller cone bit can serve as a good base for the development of new steel alloys, which can resist higher temperatures and enable effective drilling, without structural changes of steel material.

Keywords: drilling; roller cone bit; mechanism of drill bit wear; carbide coating; HV hardness; high temperature

1. Introduction

The lifetime of the roller cone bit or the time of effective drilling operations depends on the properties of the materials from which the components of the roller cone bit are made. The roller cone bit becomes worn because of the effects of the rock material through which it is drilled and the drilling regime. Owing to the wear of the bit, the penetration rate decreases.

The effective operation of the bit depends on its resistance to the factors that occur during its operation. Among the factors that have a significant impact on the effective operation of the roller cone bit, we can include the following: the steel material from which the rollers and the teeth of the bit are made, and the drilling parameters (load on the bit during drilling, torque, the number of bit rotations, and the amount and properties of the drilling fluid) in relation to the rock properties through which we drill.

We analyzed the mechanical properties of the steel material of the roller cone bit IADC 136, Ø155.57 mm (6 1/8"), which drilled through carbonate siltstone, in which sandstone sheets appear as well as rare thin layers of clay and limestone with a total length of 87.89 m.

In our research, we focused on the resistance of the steel material of the roller cone bit to the rock material.

To this end, it was necessary to identify, with scientific approaches, the causes that lead to the wear of the bit, in order to study the mechanism of flow of the drilling fluid around the rollers of the bit, which is mixed with the particles of the rock material, and to determine the weak spots on the bit that need to be technologically changed in the sense of prolonging the time of effective drilling. Extending the bit life and related efficient drilling cannot be done simply by changing one parameter, e.g., hard steel cover or tooth material itself, rather it is necessary to change and study each parameter separately for efficient drilling to achieve optimum progress.

The research on the influence of friction on the teeth material of the bit and on its stability [1,2] indicates the direction of the development of nanomaterials or nanostructured coatings, which have a low coefficient of friction and high strength and hardness, which extends the lifespan of the roller cone bit.

A number of researchers have engaged lately with the mechanism of the operation of the roller cone bit teeth to the rock material. By optimizing the shape of the teeth, the optimum rock fracture can be achieved [3–5]. The shape of the teeth, the tooth material, and the size and arrangement of the teeth on the roller cone bit must be adapted to the rock material being drilled.

The rate of penetration of the bit through the rock material as a function of the drilling regime was studied by several authors [6–11]. The influence of drilling parameters—drilling regime—such as load on the bit, number of rotations, momentum, and penetration rate of the bit into the rock, were examined.

The result of wear of the cutting mechanism on the tooth of the bit, shows that the cutting effect is greatly reduced and the geometry of the tooth of the bit is changed; therefore, a reduction in the penetration rate occurred [12–23].

An analysis of influence factors on increasing temperature during drilling on the drill bit was established by bit geometry and drilling parameters, as well as the strength and the stress state of the rock [24].

The influence of solid particles in the suspension (drilling fluid) on the erosion of steel surfaces, and consequently the loss of material and its fatigue, is significant [25–28]. The result of the erosion is loss of the steel material of the tooth. The consequence of this loss is the reduction and change in the geometry of the teeth of the roller cone bit. Because of this change in the geometry, the teeth have reduced efficiency in terms of breaking of the rock material.

An increased presence of vibrations has a considerable impact on the wear of the roller bearings. This problem has been studied by previous researchers [29,30]. In drilling technology, the usual failure of bearings depends on the following causes: vibrations of the rods during drilling, the quality of the bearing sealing, the effective lubrication of the bearings, and the quality of the bearing itself.

2. The Roller Cone Drill Bit Operation Principle

The roller cone bit contains cutting elements, i.e., teeth or inserts, which are mounted on the rollers. The rollers, which are inserted into the bearings of the bit, rotate around their axis. They are driven by the rotation of the drillstring, which drives the body of the drill bit on which the roller is mounted. Nozzles are installed on the bit body to effectively remove the rock particles from the bottom of the well and cool the bit rollers and tooth. Through the nozzles, the drilling fluid flows out from the interior of the drill rod into the bit area. Because of the reduction of the aperture represented by the ratio of the cross section of the drill bit to the cross section of the nozzles, the velocity of the outflow of the drilling fluid increases greatly, which favorably influences the flow of the outflow around the rolls,

effectively removing the drilled rock particles from the borehole and, especially in the softer poorly bonded rocks, contributing to its breaking.

The roller cone bit with steel teeth, which is the subject of study in this work, is used in softer, poorly bonded rock formations. Teeth on the rollers are large and sharp, so they can penetrate deeply into the soft rock structures where the rock is crushed and the drilled material is removed from the crushed area. In order to improve persistence and thereby prolong the effective operating time, the teeth are protected with a carbide coating. The axles of the rollers do not intersect at the point of the central axis of the bit, but have an offset according to the point of the central axis of the bit. This is usually in the range from 2° to 5°.

Through years of development of roller cone bits, several researchers explained the interrelation effect between the rock and the bit through their research. In particular, the research represented the relationship between drilling parameters and the construction of the roller cone bit. The earlier model of this correlation was presented by Galle and Woods [31], and later by Morlan [32]. Their research concerned the presentation of the rate of penetration (ROP) in softer formations in the function of weight on bit (WOB) and the number of rotations (RPM). Maurer [33,34] proposed his model as a function between the drilling regime and rock strength. The disadvantage of this model is that it has a poor estimation of the penetration rate at low loads on the bit. Bingham [35] proposed a new model for determining the penetration rate, based on a small number of laboratory data and on the estimation that, with a negligible load on the bit, the rotation of the bit progresses despite the fact that the penetration rate decreases when the rotation speed of the bit is increased. A few years later, Bourgoyne and Young [36] proposed a model for determining the penetration rate, which took into account several drilling parameters. This model was suitable for determining the penetration rate of milled tooth roller cone bits whose rollers' bearings are not sealed and the borehole is vertical. The drilling parameters that this model takes into account relate to the load on the bit, the number of rotations, and wear of teeth, and the rest as variables that are not dependent on one another. Warren [37,38] presents his model of determining the penetration rate, which takes into account the effects of the mechanical and lithological characteristics of the rock through which we drill. The model was developed using dimensional analysis, giving the corresponding curves that best match the data obtained in the laboratory. The results of this model show that the volume of the rock, which is chipped with one tooth of the roller bit, is disproportionate to the square of the load on the tooth and is inversely proportional to the square of the rock strength. Rampersad et al. [39] transformed Warren's [37,38] model by taking into account the wear of the tooth and the effect of the wedging on the part of the particles in the crater made by the tooth. In terms of the method of crushing and removing the material from the crushing site, Paul and Sikarskie [40] presented a theoretical study for a static wedge penetration model based on the Mohr–Coulomb failure criterion. Their theory shows how the tooth of the roller cone bit progresses through the crushing and shipping stages of the rock, as shown in Figure 1.

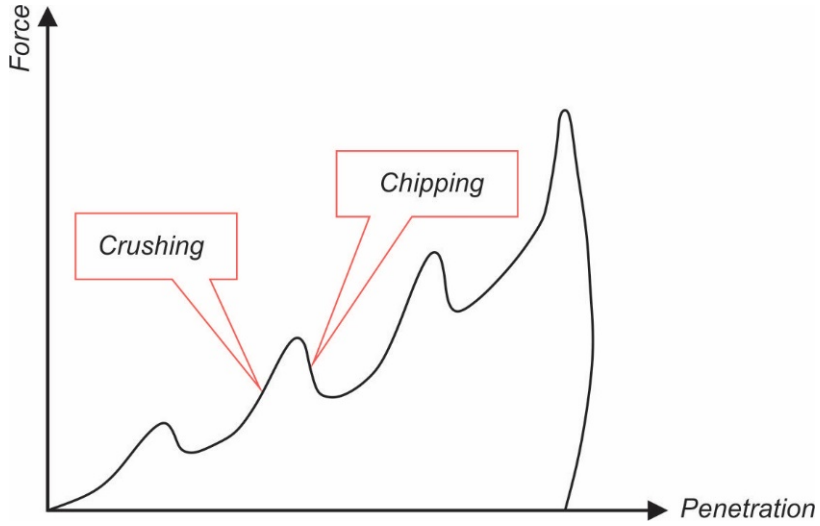


Figure 1. Progressing of the tooth of the roller cone bit through the crushing and chipping phases [40,41].

Positive slopes show elastic deformations or collapse, while negative slopes show crushing. Figure 1 shows the duration of one rolling cycle of the roller. Dutta [42] upgraded the theory of Paul and Sikarskie [40] by clarifying the crushing mechanism as an instantaneous release or energy release that involves crushing and chipping. It has been shown that the principle of demolition of the rock can be understood as the destruction of a fragile material whose breakdown cracks are the result of the operation of the cutting tool. Cheatham [43], in his study, found what load on the tooth (wedge) is needed to penetrate the rock. In his model, he assumed that the rock under the tooth is isotropic and homogeneous. This satisfied the boundaries of the Mohr–Coulomb failure criterion theory. The process of the demolition of the rock under the influence of a cutting tool—the tooth—contains the establishment of a tension state, the formation of an inelastic deformation zone, and the formation of a crater formed by a collapse wedge. The formation of the fragments of the rock resulting from the progression of the tooth into the rock is a continuous process that involves the destruction of the rock and its crushing. In the phase of crushing, the rock cracks in the area of the wedge formation. Under the influence of the progression of the tooth, tensions accumulate that lead to the fragmentation of the rock in the wedge area and, consequently, to exfoliate it from the crater. The wedge is formed along the collapse surface when a certain degree of penetration of the tooth into the rock is reached. Figure 2 shows the formation of the (i + 1) wedge after wedge i was formed.

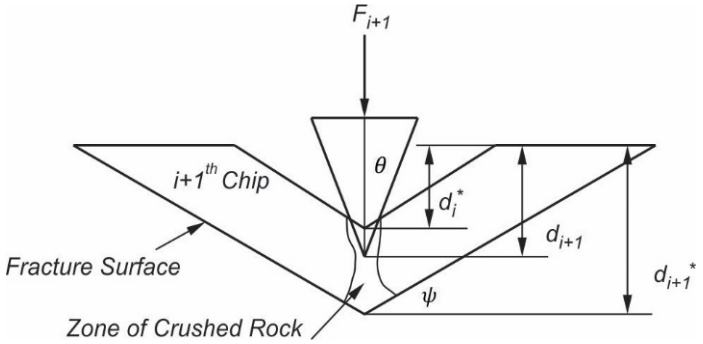


Figure 2. The model of penetration of one tooth into the rock [40].

In theory, the shear stress along the line of fracture surface is proportional to the cohesive strength of the rock, which corresponds to Mohr–Coulomb failure criterion. The angle of the rock collapse ψ,

which is characteristic of a particular type of rock material, can be shown as a function of the angle of internal friction of rock ϕ, as shown in Equation (1) and presented in Figure 3.

$$\psi = \frac{1}{2}\left(\frac{\pi}{4} - \frac{\phi}{2}\right) \tag{1}$$

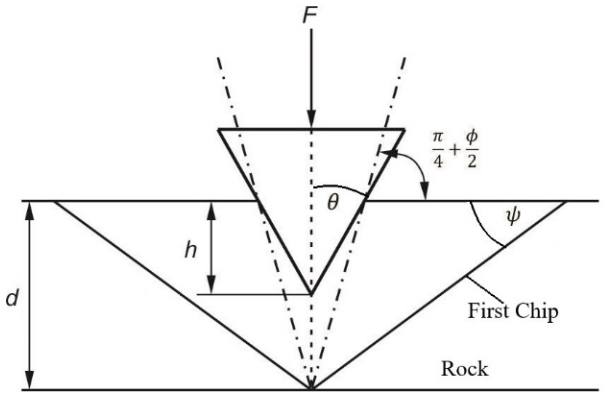


Figure 3. Formation of the first wedge under the influence of the action of a single tooth [42].

Rashidi et al. [41] developed a model for determining the rate of penetration of the roller bit based on the formation of a crater created by the individual tooth. The operation of each tooth of the bit consists of a crushing phase and a chipping of the rock, which illustrates the actual movement of the tooth on the roller of the bit.

The rock in the crater, which is removed directly by the action of the tooth, is the so-called plastic fragments of the rock, which are formed in the first stage. In the second phase or in the brittle phase, fragments of the rock are formed, which were chipped under the influence of vertical and lateral fragmentation, as shown in Figure 4.

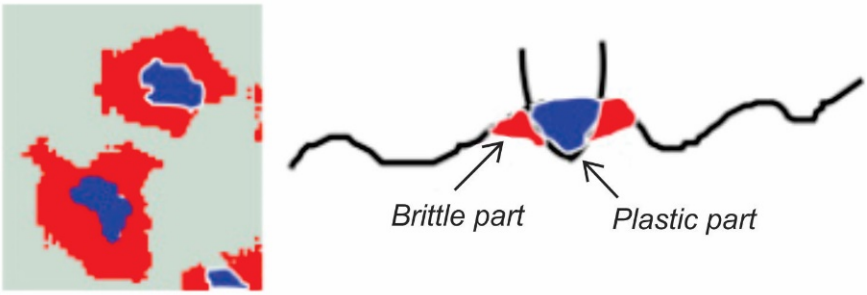


Figure 4. Scheme of rock craters generated by teeth [41].

Experimental studies have shown that the load of an individual tooth on the rock formation is linearly proportional to the depth of the cut, the length of the wedge formed, and the rock strength [44]. Further studies have shown that the load on one tooth can be expressed as a function of the projected surface of the tooth in contact with the rock, the penetration depth of the tooth, and the mechanical characteristics of the rock [6].

The load on the tooth F, which causes the penetration (h) of the tooth into the rock, is a linear combination of force acting against the surface at the tip of the tooth and force acting against the surface formed by the angled surfaces of the tooth.

For the bits that have teeth on rollers made by the same material as the roller, we could state the following [45]:

$$F = (C_1 \cdot w + C_2 \cdot h) \cdot l \cdot \sigma_p \tag{2}$$

where F is the load on a single tooth of the bit (N); C_1 is the coefficient of friction on the surface on the tooth tip (-); w is the tooth width (m); C_2 is the coefficient of friction on the tooth surface, which is in contact with the rock (-); h is the penetration depth of the tooth (m); l is the tooth length (m); and σ_p is the compressive strength of the rock (Pa).

The result of the reactive force F on the tooth of the bit, which is in contact with the rock, is equal to the load generated on the bit [41]:

$$WOB = n_t \cdot F \tag{3}$$

where WOB is weight on bit (N) and n_t is the number of teeth that are in contact with the rock.

The volume of the crater of the removed rock V_{crat} (m^3), which is created with one tooth, if we assume that the crater has a conical shape, is shown by the following equation [41]:

$$V_{crat} = \frac{1}{3} \cdot \pi \cdot r_{crat}^2 \cdot h \tag{4}$$

where r_{crat} is the crater radius (m) and h is the crater depth (m).

Assuming that the shape and associated volume of the excavated rock crater are formed according the rock fracture surface, which is formed by the angle of rock collapse ψ (°), we can state the collapse of the rock formed by the angle of the bursting rock as follows [41]:

$$tg\Psi = \frac{h}{r_{crat}}, \tag{5}$$

By following Equation (5), Equation (4) can be written as follows:

$$V_{crat} = \frac{1}{3} \cdot \pi \cdot h \cdot \left(h \cdot tg\left(\frac{\pi}{2} - \Psi \right) \right)^2 \tag{6}$$

By determining the volume of an individual crater formed by an individual tooth, the rate of penetration can be evaluated, which is defined by the volume of the rock craters on the total cutting surface of the roller cone bit in number of turns [41].

$$ROP = \frac{V_{crat} \cdot n_t \cdot RPM}{A_{bit}}, \tag{7}$$

where ROP is the rate of penetration (m/s), V_{crat} is the volume of the crater of the removed rock (m^3), RPM is the number of rotations of the bit (s^{-1}), and A_{bit} is the cutting surface of the bit (m^2).

With the advancement in the rock, the teeth of the roller cone bit wear out. To determine the wear of the bit, we focused on the parameters that influence the penetration rate (ROP) of the roller cone bit. Bourgoyne and Young [36,46] defined these as influential parameters in Equation (8).

$$ROP = f_1 \cdot f_2 \cdot f_3 \cdot f_4 \cdot f_5 \cdot f_6 \cdot f_7 \cdot f_8 \tag{8}$$

where f_1 is the effect of formation strength or rock durability, f_2 is the effect of formation depth, f_3 is the effect of formation compaction or pore pressure, f_4 is the effect of differential pressure, f_5 is the effect of bit diameter and bit weight, f_6 is the effect of rotary speed, f_7 is the effect of tooth wear, and f_8 is the effect of bit hydraulics.

We studied the wear of the roller cone bit, the appearance of damages and the change in the properties of the bit materials under the influence of the properties of the material through which it was drilled, the operational parameters (weight on bit, rotary speed, and so on), and the hydraulics of drilling fluid around the cones of the bit.

3. Materials and Methods

At the time of the investigations for the determination of the characterization of the roller cone bit wear, detailed investigations were carried out on the rock through which it was drilled, drilling parameters, and the materials from which the bit was made. To this end, we carried out an overview of the bit in the first phase, which included an overview of the condition of the bit after drilling through the rock layer according to the IADC bit dull evaluation method. In this part, we examined the state of the teeth and rollers of the rolling cone bit after drilling through familiar rock.

During drilling through known rock, the following drilling parameters were monitored:

- The load on the bit;
- The number of the bit rotations;
- The quantity of the pumped drilling fluid;
- The pressure of the pumped drilling fluid;
- The properties of the drilling fluid;
- The penetration rate;
- The length of the drilled interval.

After the removal of the bit from the well and cleaning, a visual inspection of the bit was performed along with a characterization of wear and damage according to the IADC standards.

In our investigations, we examined the various properties of the materials of the drill bit. We studied their chemical compositions, defined micro and macro structures, thermodynamic characteristics, and mechanical properties.

We performed a complete analysis of the steel materials of the roller cone bit, which included the following examinations:

- Chemical analysis of the components of the rollers and teeth with ICP (inductively coupled plasma) analyzer using ICP—OES Agillent 720;
- Analysis of the micro and macro structure of roller cone bit materials with a reflected light microscope, the Olympus BX61 and the Olympus SZ61 stereo microscope with image analysis system Analysis 6.0;
- The composition of the carbide coating of bit teeth with the XRF (X-ray fluorescence) method using a Thermo NITON XL3t XRF analyser;
- A cross-sectional view of the bit teeth with a Jeol JSM 5610 scanning electron microscope (SEM) also using EDS analysis (energy-dispersive X-ray spectroscopy);
- DSC (differential scanning calorimetry) of tooth steel and tooth carbide coating with NETZSCH STA 449 C Jupiter thermal analyser;
- A dilatometric analysis of the tooth steel and the tooth carbide coating with low temperature dilatometer Bähr-Thermoanalyse GmbH DIL 801;
- Vickers hardness tests of the teeth steel with a 100 g load with a microhardness tester Shimadzu type M.

The characteristics of the rock obtained by sampling were estimated based on the analysis by Rock Lab 1.0.

4. Results

The results of our analysis show both the way and mechanisms that cause the wear of the bit material to fail in certain rock properties in conjunction with drilling operational parameters.

In this paper, we analyzed the mechanical properties of the steel material of the IADC 136 roller cone bit Ø 155.57 mm (6 1/8"), which drilled through carbonate siltstone, in which sandstone sheets appear as well as rare thin layers of clay and limestone with a total length of 87.89 m.

4.1. Drilling

Drilling work was performed with a N-1000 drill rig made in 1992. The interval where we observed the performance of the 155.57 mm (6 1/8") roller cone drill bit included a drilling interval from 1535.15 m to 1623.04 m in depth, which amounts to 87.89 m in length. The penetration rate during the observed interval was from 0.2 to 0.4 m/h. The rest of the drilling parameters can be seen in Table 1.

Table 1. Drilling parameters.

Parameter	Value	Value	Units
Depth	1535.15–1600.00	1600.00–1623.04	m
Load on Drill Bit	30	40	kN
Rotary Speed	35	45	rpm
Pump Capacity	0.845	0.845	m^3/min
Pump Pressure	5.5	5.5	MPa

The 40 mass. % bentonite drilling fluid was used during the drilling. The drilling fluid properties are shown in Table 2.

Table 2. Drilling fluid properties.

Parameter	Value	Units
Density	1150–1170	kg/m^3
Viscosity (Fann Funnel)	45–48	s
Filtration	9.8–10	mL/30 min
Plastic Viscosity (Fann Viscosimeter)	16–18	mPas
pH	9.5	-

4.2. Rock Material

The rock material through which we drilled was periodically sampled from drilling fluid. Each sample of rock material was examined and compared to a predetermined lithological column, which was made on the basis of the results of geophysical and laboratory measurements in the surrounding wells.

As for the lithology of the drilled interval; the silty claystone is dominant, and in the lower and upper part of the sequence, layers of carbonate siltstone with sandstone sheets and thin layers of clay and limestone appear.

The geomechanical properties of the drilled wellbore section were evaluated on the basis of experience. Strength properties were evaluated using Hoek–Brown's criterion with RockScience software, Rock Lab 1.0 (Figures 5 and 6).

The estimated values for the carbonate siltstone are shown in Table 3.

The estimated values for limestone are shown in Table 4.

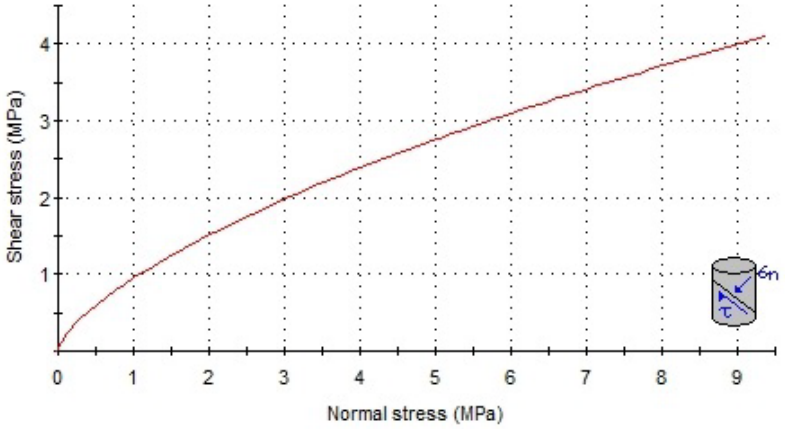


Figure 5. Estimated value shear stress–normal stress for carbonate siltstone.

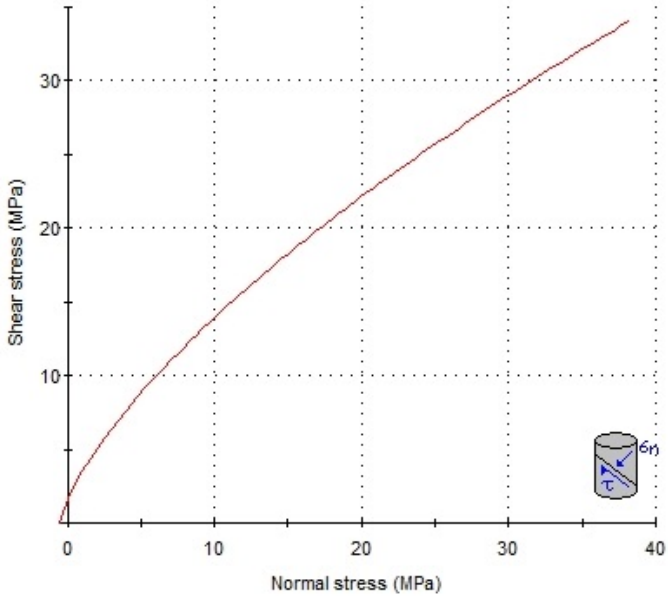


Figure 6. Estimated value shear stress–normal stress for limestone.

Table 3. Results of the geomechanical properties of carbonate siltstone.

Parameter	Value	Units
Cohesion	0.722	MPa
Angle of Internal Friction	20.94	°
Elastic Module	9375	MPa
Compressive Strength	25	MPa

Table 4. Results of the geomechanical properties of limestone.

Parameter	Value	Units
Cohesion	5.50	MPa
Angle of Internal Friction	38.42	°
Elastic Module	28125	MPa
Compressive Strength	75	MPa

4.3. Roller Cone Bit

After drilling, the drill bit was examined using the IADC dull grading system. We found that the teeth of the bit were evenly worn. Some individual teeth were broken. There are no apparent erosion effects of the rock particles in the drilling fluid that would erode the steel material of the bit. The results of dull inspection of the drill bit can be seen in Table 5.

Table 5. Results of the dull inspection of drill bit according to the IADC dull grading system. BT, broken teeth; CT, chipped tooth; FC, flat crested wear.

Cutting Structure				B	G	Remarks	
Inner Rows	Outer Rows	Dull Char.	Location	Bearings/Seals	Gauge	Other Dull Char.	Reason Pulled
T2	T2	FC	A	E	I	BT, CT	PR

In Figure 7, we can see the condition of the roller cone bit after the drilled interval of 87.89 m.



Figure 7. Drill bit condition after the drilled interval of 87.89 m.

After visual dull inspection, we prepare the teeth of the roller cone bit for the microscopic analyses as shown in Figure 8.

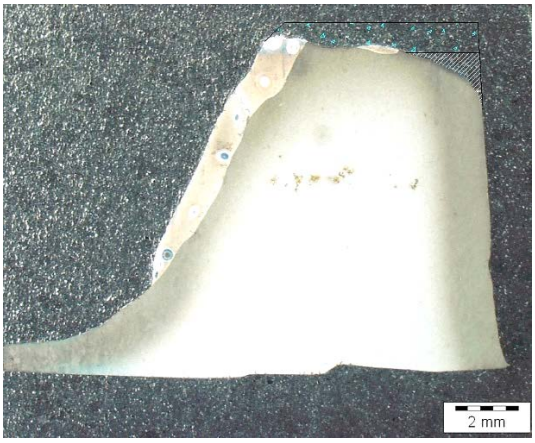


Figure 8. Macroscopic cross-sectional view through the bit tooth, with a reconstruction of the original geometry.

4.4. Tooth Steel Material Analyses

We examined the steel material and the carbide coating of the teeth.

An investigation of the chemical composition of the teeth steel was performed on an optical emission spectrometer (ICP). The results of the chemical composition of the investigated steel (body) can be seen in Table 6.

Table 6. Chemical analysis of the investigated tooth steel (body).

Element	mas. %
C	0.17
Si	0.26
Mn	0.79
P	0.011
S	0.016
Cr	0.60
Ni	0.74
Cu	0.27
Mo	0.50

The results of chemical analysis (Table 6) show that, in this case, the steel material of the tooth body is the so-called chromium, molybdenum, nickel low alloy steel often used for case-hardened parts.

Using SEM, we metallographically analysed the steel base of the tooth (chromium, molybdenum, nickel low alloy steel), the contact area between the tooth body and the carbide coating, and the carbide coating itself. By EDS analysis, we determined the chemical composition of the steel of each component of the tooth. Figure 9 (SEM) shows the areas where we perform metallographic tests on the teeth. Tables 7–10 show the results of EDS analyses for each individual analysed component.

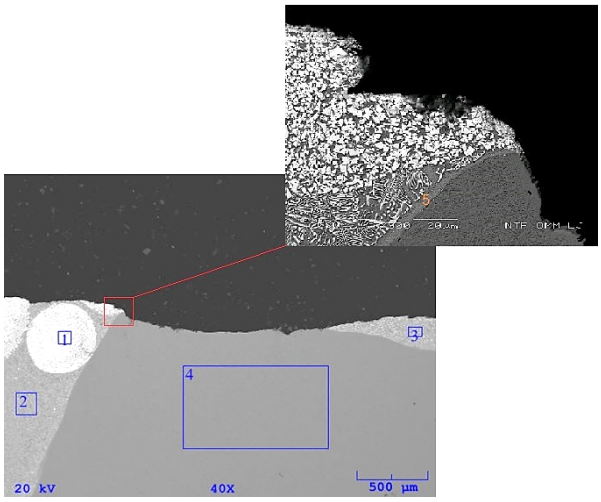


Figure 9. Scanning electron microscope (SEM) image of bit tooth: 1—carbide material, 2 and 3—carbide coating matrix, 4—tooth body, and 5—mixed zone.

Table 7. The elemental composition of carbide material (1—Figure 9).

Element	Concentration	
	at. %	wt. %
Fe	0.807	0.962
Co	42.380	19.500
W	55.415	79.539

Table 8. The elemental composition of the carbide coating matrix (2—Figure 9).

Element	Concentration	
	at. %	wt. %
Mn	0.892	0.699
Fe	86.096	68.599
Ni	1.921	1.608
W	1.709	29.094

Table 9. The elemental composition of the carbide coating matrix (3—Figure 9).

Element	Concentration	
	at. %	wt. %
Mn	1.269	0.995
Fe	86.117	68.616
Ni	1.511	1.265
W	11.103	29.124

Table 10. The elemental composition of the tooth body (4—Figure 9).

Element	Concentration	
	at. %	wt. %
Si	0.531	0.267
Mn	0.660	0.649
Fe	95.427	95.385
Ni	3.164	3.323
Mo	0.218	0.375

The elemental composition of the carbide material (1—Figure 9) determined by the EDS is shown in Table 7.

The elemental composition of the carbide coating matrix (2—Figure 9) determined by the EDS is shown in Table 8.

The elemental composition of the carbide coating matrix (3—Figure 9) determined by the EDS is shown in Table 9.

The elemental composition of the tooth body (4—Figure 9) determined by the EDS is shown in Table 10.

We performed a simultaneous thermal analysis (STA) (Figure 10) of the steel sample of the tooth body. The curve shows that an eutectoid transformation in its solid state starts at a temperature of 693.9 °C. There is an endothermic peak. The process ends at 800 °C when the metal matrix (iron) is transformed into a gamma-phase iron structure also known as austenite (γ-Fe). The temperature of 1407.2 °C is the low temperature when the eutectics began to melt. At 1474.5 °C, the rest of metal matrix (austenite) started to melt. The temperature of 1474.5 °C is also the solidus temperature of steel from which the tooth body is made.

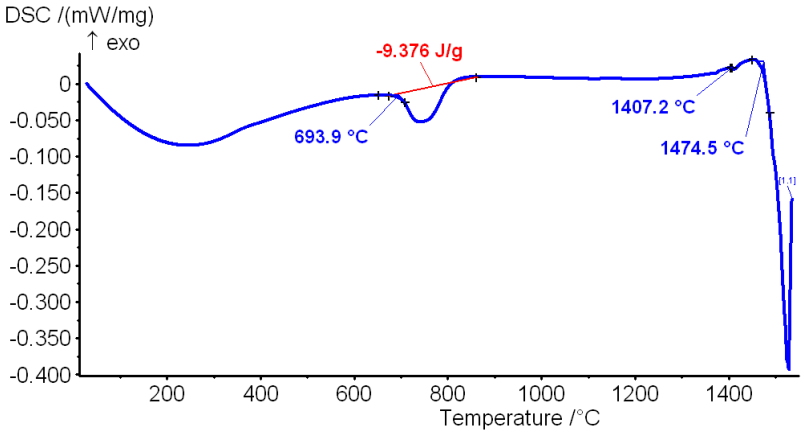


Figure 10. Differential scanning calorimetry (DSC) heating curve of the steel of the tooth body.

The DSC heating curve of the carbide coating of the teeth in roller cone bit is shown in Figure 11. The carbide coating contains a thin layer of the mixing zone. The mixing zone is the area formed during the welding of the carbide protection to the tooth. It contains the characteristics of steel of the tooth body and carbide coating. At the temperature of 692.5 °C, the start of eutectoid transformation was detected. This transformation is related to the layer of the mixing zone. Therefore, this curve is not typical for carbide alloys. At a temperature of 1467.3 °C, the first melting was detected.

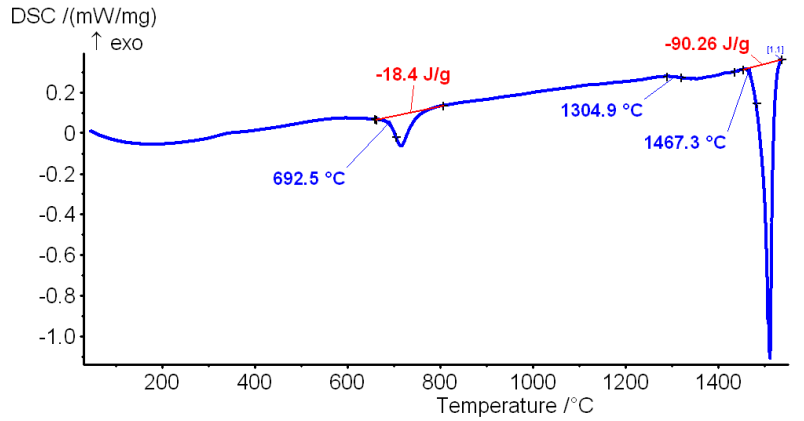


Figure 11. DSC heating curve of carbide coating.

Figure 12 shows the dilatometric curve of the steel of the tooth body and carbide coating. From the steel of the tooth body, during the heating curve, it is evident that the temperature of the eutectoid transformation is increasing linearly. The slope of the curve corresponds to the linear expansion coefficient for chromium, molybdenum, and nickel low alloy steel, while the slope of heating curve of the sample of the carbide coating, which contains a thin layer of the mixing zone, is lighter. A lower curve angle of the carbide coating sample with a thin layer of the mixing zone is the result of a lower temperature expansion coefficient.

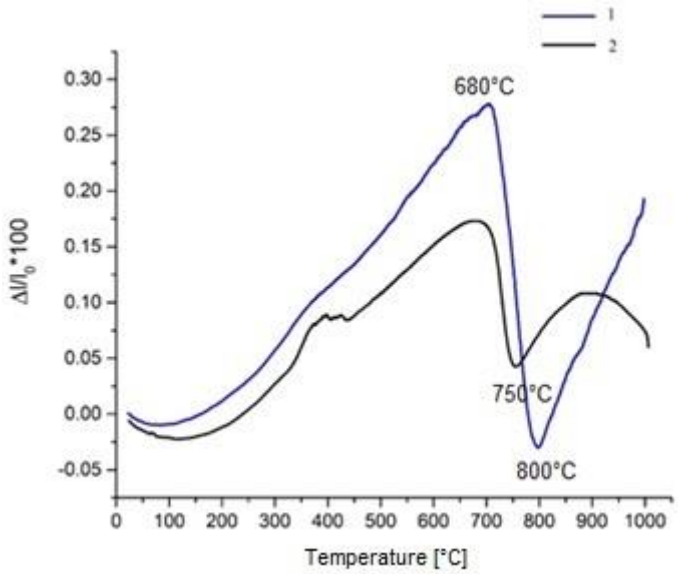


Figure 12. Dilatometric heating curve of the steel of the tooth and carbide coating: 1—tooth steel material, 2—carbide coating.

In view of the fact that, during drilling, despite intense cooling, the temperatures can reach up to 500 °C locally, the curves show that the difference between the expansion properties is 0.05%. Because of this difference, the mixing zone is the preferred area for the formation of internal tension, and thus the formation and spread of microfractures. The diagram shows the beginning of the eutectoid transformation sample of the steel from the tooth body, which begins at 680 °C (A_{c1}) and ends at a temperature of 800 °C (A_{c3}). For the sample of the carbide coating that contains a thin layer of the mixing zone, the temperature of the start of the eutectoid transformation is 750 °C. On the curve, the sample of the carbide coating contains a thin layer on the mixing zone, a deviation can be observed, which can be associated with the eutectoid transformation of the thin layer of the mixing zone, but the temperature is slightly higher. The cause of this higher temperature can be found in the chemical composition of the mixing zone.

To determine the changes in the hardness properties of the tooth, as a result of the effects of drilling, a Vickers hardness test was carried out. The measurement points are shown in Figure 13 (Figure 14) and the results of the tests are provided in Table 11. The average hardness of the steel of the teeth's body is 433.5184 HV. The average hardness of the steel at the tip of the teeth is much higher, and it is 594.5670 HV. As expected, the hardness of the carbide coating is much higher and reaches a value up to 1471.137 HV.

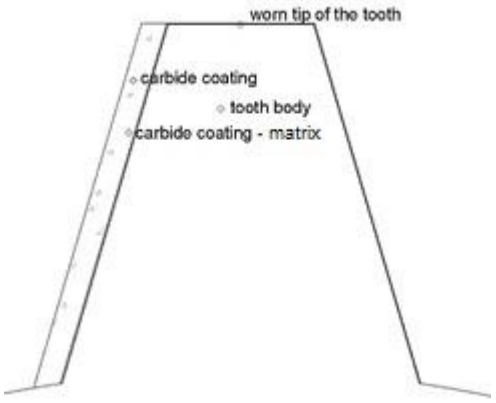


Figure 13. Display of measurement positions of micro hardness tests on the tooth.

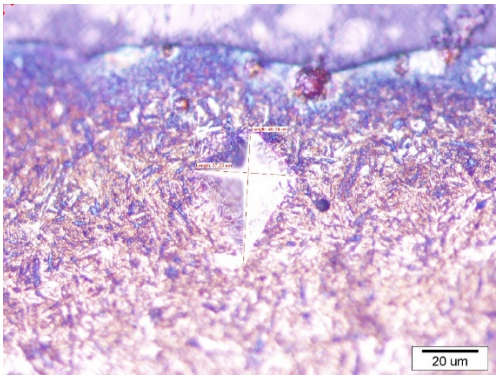


Figure 14. Vickers hardness test on the tip of the tooth.

Table 11. Vickers hardness test results.

Diagonals (μm) d1	d2	Hardness (HV0.5)	Average	Note
37.23	46.24	532.3198	594.5670	Tip of the tooth
36.22	37.55	681.5125		
36.4	40.81	622.1374		
37.99	41.33	589.4786		
37.54	41.66	591.2662		
37.43	39.54	626.0232		
37.57	39.86	618.6071		
36.33	42.41	598.1947		
38.87	42.45	560.8396		
38.48	42.45	566.2580		
39.01	42.84	553.6000		
44.99	47.95	429.3664	433.5184	Tooth body
44.44	48.37	430.5701		
44.61	47.78	434.4937		
44.09	47.10	446.0042		
45.14	48.04	427.1575		
33.28	37.13	748.1087	784.1543	Carbide coating—matrix
31.73	34.04	857.3887		
33.64	36.53	753.2349		
34.58	36.51	733.8654		
30.41	36.51	828.1739		
24.67	25.96	1446.830	1458.984	Carbide coating—base
24.43	25.78	1471.137		

5. Discussion

While monitoring the operational parameters during drilling, it was determined that the roller cone bit was not loaded in accordance with the manufacturer's recommendations, which recommend that the load on the bit is in range between 15 and 27 kN. The load on the bit during drilling was between 30 and 40 kN. Moreover, the number of bit rotations was too low, as they ranged from 35 to 45 rpm. The recommended number of rotations for this bit type is between 60 and 100 rpm.

It can be noted that the bit was overloaded with weight and the number of bit turns was too low.

After cleaning, the damage of the bit was mainly reflected in the wear of the tooth tip (according to IADC: FC (flat crested wear)), which was expressed on all the teeth of the bit (Figure 15). Some teeth were chipped (according to IADC: CT (chipped tooth)), and some were broken (according to IADC: BT (broken teeth)).

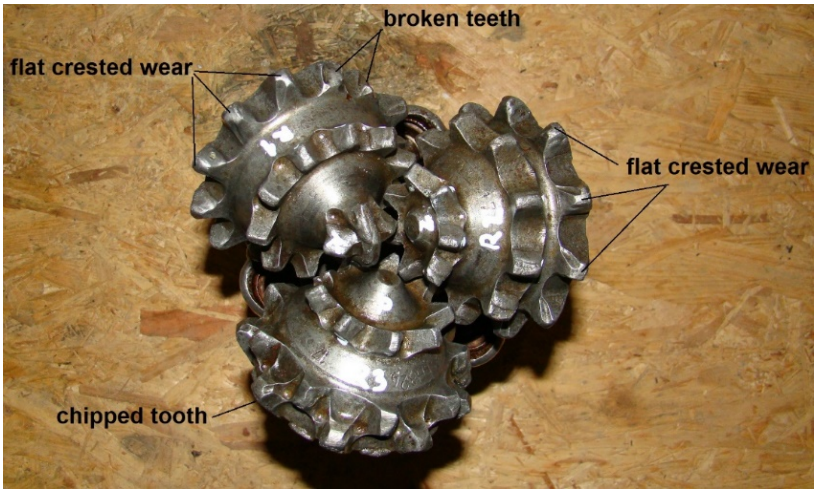


Figure 15. Characteristic dull of the roller cone bit.

In the examination of the microscopic image, it was evident that the tops of the teeth were exposed to high temperatures and stresses. The influence of high temperatures and loads is shown in Figure 16.

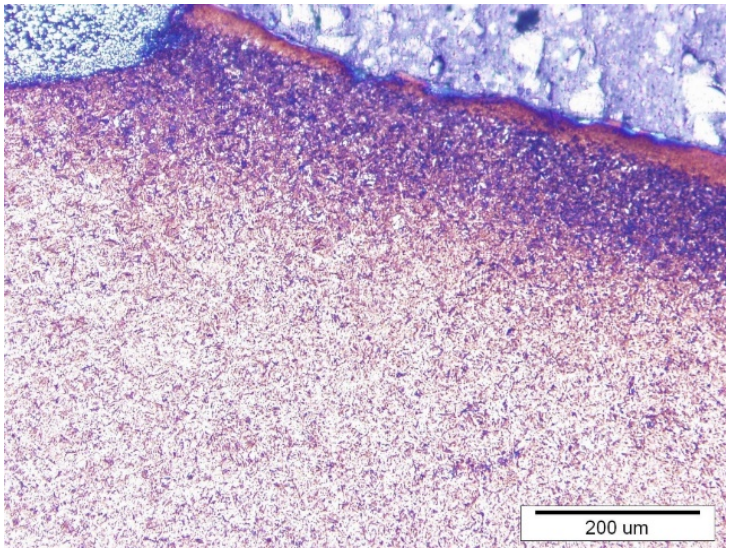


Figure 16. Microscopic photo of the tip of the tooth, etched with Nital.

Figure 16 shows the tip of the tooth that was in contact with the rock. We can see changes in the color of the steel, which changes from top to bottom in shades of blue (at the point of contact between the rock and steel) to shades of brown, which changes the light from the top downwards.

Because of the apparent color change that was previously observed under the optical microscope, the sample was examined by a scanning electron microscope (SEM). A characteristic view of the microstructure of the area with an SEM is shown in Figure 17.

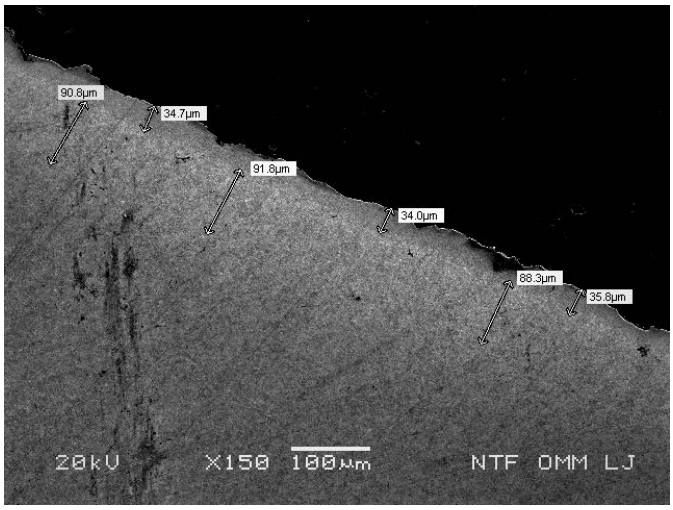


Figure 17. A view at the working surface that was in contact with the rock.

Figure 17 shows the state of the tip of the tooth that was in contact with the rock during drilling. A change in the microstructure of the steel on the surface was observed. The change in the steel structure is noticeable in two layers. The first layer, where the change is noticeable, is up to a thickness of 36 µm. The second layer, where the change in the microstructure is less expressed, but still noticeable, moves to a depth of up to 92 µm.

The change in the steel microstructure of the tooth was due to the high temperatures and mechanical loads that occurred during drilling when the tip of the tooth was in contact with the rock. When turning the roller cone bit around on its axis, the teeth were cooled. The teeth, which are not in contact with the rock, were cooled by the drilling fluid that comes from the nozzles of the bit. In this situation, there is a temperature change on the surface of the teeth when their temperature is very high and they are washed by drilling fluid with a lower temperature. Another reason for microstructural changes in the steel can be found in the fact that the bit was overloaded during drilling and the number of turns was too low in relation to the load. The consequence of such a drilling regime is increasing temperature of the material at the top of the tooth, which, in connection with the load, has led to the hardening of the material at the tip of the teeth. For this reason, the hardness of the steel material increased. The measured hardness (according to Vickers) was, at this point, higher, on average, by approximately 160 HV than the hardness of the steel material in the center of the tooth.

With differential scanning calorimetry (DSC), we found that the temperature of the eutectoid point is 699.2 °C or its completion at a temperature of 800 °C. Because of the intensive cooling of teeth under the influence of the drilling fluid, the microstructural change process proceeded only in the steel layer up to a depth of 92 µm. Microstructural changes are noticeable only at the top of the teeth, while at the sides, there were no changes observed.

The changes in steel microstructure occurred mainly as a result of excessive working temperatures and loads for the selected steel. As proved by DSC and dilatometric analysis, for the selected steel, the temperature at the start of the transformation from ferrite to austenite is approximately 680 °C. This means that the temperature of 680 °C (A_{c1}) represents a point where the recrystallization of steel accelerates rapidly. The recrystallization temperature for steel, if it is calculated for the information, is somewhere around $0.4 \times T_L$ (T_L = liquidus temperature, °C) [47]. Using the Thermo-Calc software, which is used for thermodynamic modeling of phase of equilibrium, we calculated the liquidus temperature, which was 1511 °C for the selected steel. Therefore, the temperature of the recrystallization for the analyzed steel is approximately 604 °C. We also calculated the equilibrium eutectoid temperature A_{e1} and transition temperature A_{e3} using Thermo-Calc. The first one was at 685 °C and the other at 811 °C. The calculated values are very well matched with the values obtained from the dilatometric

analysis of the steel (680 °C and 800 °C), assuming, of course, that the temperatures obtained from the calculation are in equilibrium. This confirmed the results of the dilatometric analysis.

Owing to the influence of high temperatures and rapid cooling, there was a disintegration of the carbide coating on the top of the teeth. With a low temperature dilatometric test, the difference between the temperature extensibility coefficients of the steel material and the carbide form was found. This difference is important because of the increase in internal tension in the mixed zone. The mixed zone is formed by welding the carbide coating on the tooth steel and represents a mixture of dissolved steel material of the tooth and carbide coating (Figure 18). In the mix zone, during the processes of heating and cooling, because of the different temperature coefficients of materials, internal tension starts to increase, which leads to the initiation and propagation of cracks.

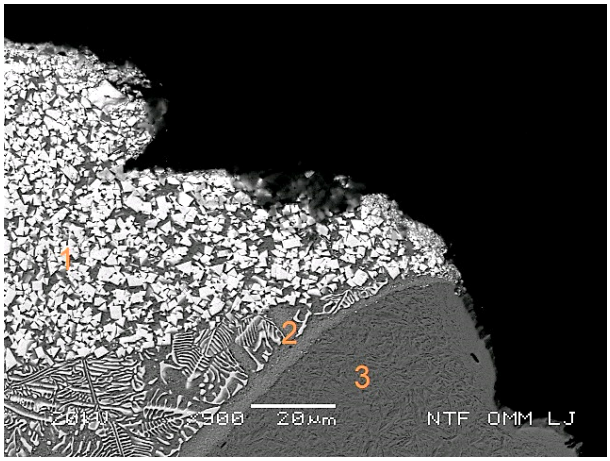


Figure 18. Display of tooth steel material: 1—carbide coating, 2—mixed zone, 3—tooth steel (body).

At the edges of the teeth, cracks were observed that passed through the carbide coating to the steel of the tooth (body) (Figure 19). The occurrence of such cracks can be attributed to the excessive load on the bit during drilling and the accumulation of stress due to the loading of the bit by weight. The carbide coating is tough and erosion-resistant, but brittle, causing them to burst with excessive loads and transverse forces. Owing to the formation of such cracks at the edges of the teeth, there was a deviation of the carbide coat, which was expressed as a chipped tooth (CT, according to the IADC classification).

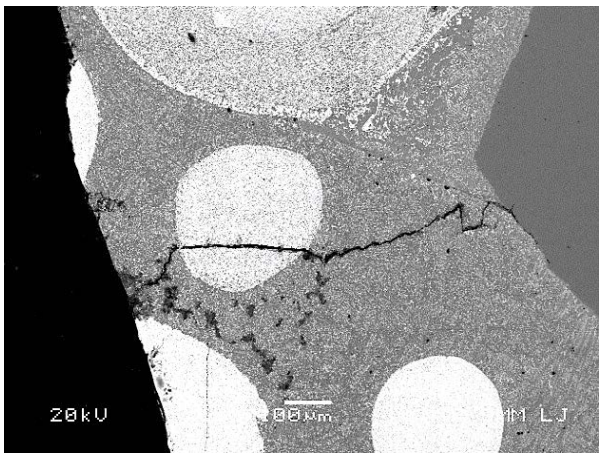


Figure 19. Display of cracks through carbide coating.

The erosion effect caused by aggressive particles in the drilling fluid has not yet been expressed, as only a short interval of 87.89 m was drilled with this bit. In microscopic images, smaller erosion micro channels can be seen, which are not largely expressed (Figure 20). Erosion micro channels occur

only in the area at the tip of the tooth. There are no erosion channels along the edges of the teeth, which are not protected by carbide coatings, which can be partly attributed to the geometry of the teeth, because their sides are quite steep, which leads to the drilling fluid with abrasive particles leaving the tooth area in a short period of time.

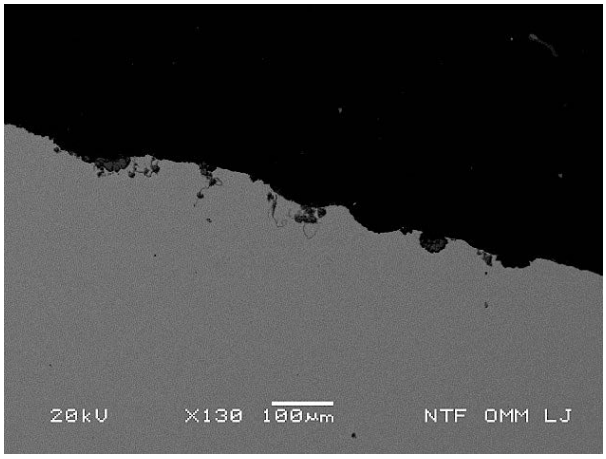


Figure 20. Erosion channels at the top of the tooth.

6. Conclusions

In this article, we described the wear of the IADC 136 roller cone bit, which was drilling in known rock material. The characterization of bit wear was made by an analysis of different metallurgical properties of the steel bit and carbide coating, which was related to the operational parameters and rock material properties. During drilling, the teeth of the bit are heated in contact with the rock, and then cooled because of the influence of the drilling fluid. At this stage, there is a compressive load on both the steel tooth and the carbide coating. Internal stresses in the materials of the bit teeth, resulting from the load on the bit, can be extended through the elastic zone and reach the plastic zone, which results in a local disintegration of the carbide coating and locally increase in the hardness of the steel material.

With an IADC 136, Ø155.57 mm (6 1/8") roller cone bit, an interval of 87.89 m was drilled in a carbonate siltstone with sandstone sheets and thin layers of clay and limestone. The wear of the teeth of the roller cone bit was mainly observed as the wear of the tooth tip. In the systematical examination of the steel structure of the teeth and carbide coating, it was found that, because of the influence of high deformations, the microstructure of the steel material at the top of the tooth was partially changed. This change, reflected by the increase of the hardness of the steel material, was higher at the tip of the tooth that was in contact with the rock than the tooth's body by 160 HV. The change in the hardness of the steel material, expressed as a layer parallel to the tooth tip, extends to a depth of about 36 µm. The formation of this layer with a higher level of hardness can be explained by the implementation of weight on the bit (WOB), which was higher than the recommended and relatively low rotation (RPM), which was lower than recommended. The increase in the temperature of the tooth material during drilling was due to excessive loads and inefficient cooling, which led to micro fatigue reaching the plastic zone of the steel material at the tooth tip. The tip of the tooth, owing to friction along the rock, was worn through a modified microstructure, and a new layer with a modified microstructure was periodically beneath it.

From this, we can conclude that making the correct choice for the roller cone bit for a particular type of rock and operational parameters is recommended (WOB, RPM, drilling fluid), because it has a significant influence on the wear of the roller cone bit, and thus the extension or reduction of the effective operating time of the roller cone bit.

The results of our investigation of the roller cone bit materials can be a good base for the development of new steel alloys, which can resist higher temperatures and enable effective drilling, without structural changes of steel material.

Simultaneously with the development of suitable steel alloys that will allow drilling at higher temperatures without structural changes, it is necessary to pay attention to research that will increase the reliability and extend the lifetime of roller bearings. In this research, attention should be focused on the effects of vibration on bearings.

Moreover, the modern 3D scanning technique can be used to assess the wear of the drill bits. The results of the 3D scan will give an accurate and clear picture of the degree and method of wear of the teeth, rollers, and body of the roller cone bits.

Author Contributions: Conceptualization, J.Š., P.M., and Ž.V.; methodology, J.Š. and P.M.; software, T.B. and J.Š.; validation J.Š., T.B., P.M., and Ž.V.; formal analysis, J.Š., T.B., and P.M.; investigation, J.Š., T.B., and B.J.; resources, J.Š. and Ž.V.; data curation, J.Š., T.B., and B.J.; writing—original draft preparation, J.Š.; writing—review and editing, B.J. and T.B.; visualization, J.Š. and B.J.; supervision, P.M. and Ž.V. All authors have read and agreed to the published version of the manuscript.

Funding: This research received no external funding.

Conflicts of Interest: The authors declare no conflict of interest.

References

1. Peter, W. Wear-Resistant NanoComposite Stainless Steel Coatings and Bits for Geothermal Drilling. Presented at the Geothermal Technology Program, The Antares Group, Crystal City Hyatt, Alexandria, VA, USA, 18–20 May 2010.
2. Eremin, E.N.; Yurov, V.M.; Guchenko, S.A.; Laurynas, V.C.; Kasymov, S.S. Antifriction Superhard Coatings for Drill Bits and Boring Cutters. *Procedia Eng.* **2016**, *152*, 608–612. [CrossRef]
3. Jaime, M.C.; Zhou, Y.; Lin, J.S.; Gamwo, I.K. Finite element modeling of rock cutting and its fragmentation process. *Int. J. Rock Mech. Min. Sci.* **2015**, *80*, 137–146. [CrossRef]
4. Yang, C.; Jiang, J.; Cao, P.; Wang, J.; Fan, X.; Shang, Y.; Talalay, P. Assessing the efficiency of carbide drill bits and factors influencing their application to debris-rich subglacial ice. *Polar Sci.* **2017**, *13*, 50–55. [CrossRef]
5. Hu, Q.; Zhu, H.; Ren, H. Research on shape parameters of circular arc disc teeth for three-cone bit. *Petroleum* **2018**, *4*, 108–114. [CrossRef]
6. Ma, D.K.; Yang, S.L. Kinematics of the Cone Bit. *Soc. Pet. Eng. J.* **1985**, *25*, 321–329. [CrossRef]
7. Naganawa, S. Dynamics modeling of roller cone bit axial vibration. *J. Jpn. Assoc. Pet. Technol.* **2005**, *70*, 333–346. [CrossRef]
8. Naganawa, S. Feasibility study on roller-cone bit wear detection from axial bit vibration. *J. Pet. Sci. Eng.* **2012**, *82–83*, 140–150. [CrossRef]
9. Njobuenwu, D.O.; Wobo, C.A. Effect of drilled solids on drilling rate and performance. *J. Pet. Sci. Eng.* **2007**, *55*, 271–276. [CrossRef]
10. Saeidi, O.; Torabi, S.R.; Ataei, M.; Rostami, J. A stochastic penetration rate model for rotary drilling in surface mines. *Int. J. Rock Mech. Min. Sci.* **2014**, *68*, 55–65. [CrossRef]
11. Stupina, A.A.; Shigin, A.O.; Shigina, A.A.; Karaseva, M.V.; Korpacheva, L.N. Control and Management by Resource of Rolling Cutter Bits in Drilling Rock Massif. *Middle East J. Sci. Res.* **2014**, *21*, 84–90.
12. Geoffroy, H.; Nguyen Minh, D. Study on interaction between rocks and worn PDS'S cutter. *Int. J. Rock Mech. Min. Sci.* **1997**, *34*, 95. [CrossRef]
13. Zhou, Y. Numerical Modeling of Rock Drilling with Finite Elements. Ph.D. Thesis, University of Pittsburgh, Pittsburgh, PA, USA, 2013.
14. Dagrain, F.; Lamine, E.; Delwiche, R.; Golard, N. Characterization of the performances of small diameter drill bits for the optimization of the drilling parameters. In Proceedings of the 2nd International Conference on Stone and Concrete Machining (ICSCM), Dortmund, Germany, 14–15 November 2013.
15. Kanyanta, V.; Dormer, A.; Murphy, N.; Ivankovic, A. Impact fatigue fracture of polycrystalline diamond compact (PDC) cutters and the effect of microstructure. *Int. J. Refract. Met. Hard Mater.* **2014**, *46*, 145–151. [CrossRef]

16. Günen, A. Micro-Abrasion Wear Behavior of Thermal-Spray-Coated Steel Tooth Drill Bits. *Acta Phys. Pol. A* **2016**, *130*, 217–222. [CrossRef]
17. Karasawa, H.; Ohno, T.; Miyazaki, K.; Eko, A. Experimental results on the effect of Bit wear on torque response. *Int. J. Rock Mech. Min. Sci.* **2016**, *84*, 1–9. [CrossRef]
18. Yahiaoui, M.; Paris, J.Y.; Delbé, K.; Denape, J.; Gerbaud, L.; Dourfaye, A. Independent analyses of cutting and friction forces applied on a single polycrystalline diamond compact cutter. *Int. J. Rock Mech. Min. Sci.* **2016**, *85*, 20–26. [CrossRef]
19. Al-Sudani, J.A. Real-time monitoring of mechanical specific energy and bit wear using control engineering systems. *J. Pet. Sci. Eng.* **2017**, *149*, 171–182. [CrossRef]
20. Botti, L.; Mora, C.; Antonucci, A.; Carty, P.; Barr, A.; Rempel, D. Carbide-tipped bit wear patterns and productivity with concrete drilling. *Wear* **2017**, *386–387*, 58–62. [CrossRef]
21. Jones, H.G.; Norgren, S.M.; Kritikos, M.; Mingard, K.P.; Gee, M.G. Examination of wear damage to rock-mining hardmetal drill bits. *Int. J. Refract. Met. Hard Mater.* **2017**, *66*, 1–10. [CrossRef]
22. Olsson, M.; Yvell, K.; Heinrichs, J.; Bengtsson, M.; Jacobson, S. Surface degradation mechanisms of cemented carbide drill buttons in iron ore rock drilling. *Wear* **2017**, *388–389*, 81–92. [CrossRef]
23. Timonin, V.V.; Smolentsev, A.S.; Shakhtorin, O.; Polushin, N.I.; Laptev, A.I.; Kushkhabiev, A.S. Causes of wear of PDC bits and ways of improving their wear resistance. In Proceedings of the All-Russian Conference on Challenges for Development in Mining Science and Mining Industry devoted to the 85th anniversary of Academician Mikhail Kurlenya, Novosibirsk, Russia, 3–6 October 2016.
24. Qiu, P.; Li, X.; Ning, J.; Wang, J.; Yang, S. Study on Thermal Energy Conversion Theory in Drilling Process of Coal and Rock Mass with Different Stresses. *Energies* **2019**, *12*, 4282. [CrossRef]
25. Neville, A.; Hodgkiess, T. Characterisation of high-grade alloy behaviour in severe erosion-corrosion conditions. *Wear* **1999**, *233–235*, 596–607. [CrossRef]
26. Neville, A.; Reyes, M.; Hodgkiess, T.; Gledhill, A. Mechanisms of wear on a Co-base alloy in liquid-solid slurries. *Wear* **2000**, *238*, 138–150. [CrossRef]
27. Zhao, J.; Zhang, G.; Xu, Y.; Wang, R.; Zhou, W.; Yang, D. Experimental and theoretical evaluation of solid particle erosion in an internal flow passage within a drilling bit. *J. Pet. Sci. Eng.* **2018**, *160*, 582–596. [CrossRef]
28. Vryzas, Z.; Kelessidis, C.V. Nano-Based Drilling Fluids: A Review. *Energies* **2017**, *10*, 540. [CrossRef]
29. He, W.; Chen, Y.; He, J.; Xiong, W.; Tang, T.; OuYang, H. Spherical contact mechanical analysis of roller cone drill bits journal bearing. *Petroleum* **2016**, *2*, 208–214. [CrossRef]
30. Zmarzły, P. Influence of the internal clearance of ball bearings on the vibration level. *Eng. Mech.* **2018**, *24*, 961–964.
31. Galle, E.M.; Woods, H.B. Variable weight and rotary speed for lowest drilling cost. Presented at the 20th Annual Meeting of AAODC (American Association of Oilwell Drilling Contractors), New Orleans, LA, USA, 25–27 September 1960.
32. Morlan, E.A. Boring large hole mine openings. Presented at the Annual Meeting of SME–AIME (Society for Mining, Metallurgy and Exploration–American Institute of Mining, Metallurgical and Petroleum Engineers), St. Louis, MO, USA, 25– 28 February 1961.
33. Maurer, W.C. The "Perfect-Cleaning" Theory of Rotary Drilling. *J. Pet. Technol.* **1962**, *14*, 1270–1274. [CrossRef]
34. Maurer, W.C. Bit-Tooth Penetration Under Simulated Borehole Conditions. *J. Pet. Technol.* **1965**, *17*, 1433–1442. [CrossRef]
35. Bingham, M.G. *A New Approach to Interpreting Rock Drillability*; Petroleum Publishing Co.: Tulsa, OK, USA, 1965.
36. Bourgoyne, A.T.; Young, F.S. A Multiple Regression Approach to Optimal Drilling and Abnormal Pressure Detection. *Soc. Pet. Eng. J.* **1974**, *14*, 371–384. [CrossRef]
37. Warren, T.M. Drilling Model for Soft-Formation Bits. *J. Pet. Technol.* **1981**, *33*, 963–970. [CrossRef]
38. Warren, T.M. Penetration Rate Performance of Roller Cone Bits. *Soc. Pet. Eng.* **1987**, *2*, 9–18. [CrossRef]
39. Rampersad, P.R.; Hareland, G.; Boonyapaluk, P. Drilling Optimization Using Drilling Data and Available Technology. Presented at the SPE (Society of Petroleum Engineers) Latin America/Caribbean Petroleum Engineering Conference, Buenos Aires, Argentina, 27–29 April 1994.
40. Paul, B.; Sikarskie, D.L. A preliminary model for wedge penetration in brittle materials. *Trans. Am. Inst. Min. Eng.* **1965**, *232*, 373–383.

41. Rashidi, B.; Hareland, G.; Wu, Z. Performance, simulation and field application modeling of rollercone bits. *J. Pet. Sci. Eng.* **2015**, *133*, 507–517. [CrossRef]
42. Dutta, P.K. A theory of percussive drill bit penetration. *Int. J. Rock Mech. Min. Sci. Geomech. Abstr.* **1972**, *9*, 543–567. [CrossRef]
43. Cheatham, J.B. An analytical study of rock penetration by a single bit tooth. In Proceedings of the 8th Drilling and Blasting Symposium, Minnesota, MN, USA, 2–4 October 1958.
44. Evans, I.; Murrell, S. Wedge penetration into coal. *Colliery Eng.* **1962**, *39*, 11.
45. Hareland, G.; Wu, A.; Rashidi, B. A New Drilling Rate Model for Tricone Bit and Its Application to Predict Rock Compressive Strength. Presented at the 44th US Rock Mechanic Symposium and 5th U.S.-Canada Rock Mechanics Symposium, Salt Lake City, UT, USA, 27–30 June 2010.
46. Bourgoyne, A.T.; Millheim, K.K.; Chenevert, M.E.; Young, F.S. Rotary Drilling Bits. In *Applied Drilling Engineering*; SPE: Richardson, TX, USA, 1991; pp. 190–245.
47. Totten, G.E. *Steel Heat Treatment: Metallurgy and Technologies*, 2nd ed.; CRC Press: Boca Raton, FL, USA, 2006.

Publisher's Note: MDPI stays neutral with regard to jurisdictional claims in published maps and institutional affiliations.

© 2020 by the authors. Licensee MDPI, Basel, Switzerland. This article is an open access article distributed under the terms and conditions of the Creative Commons Attribution (CC BY) license (http://creativecommons.org/licenses/by/4.0/).